Digital Object Identifier: 10.1109/ULTSYM.2008.0012

An Inertial-Optical Tracking System for Portable, Quantitative, 3D Ultrasound

A. M. Goldsmith, P. C. Pedersen
Worcester Polytechnic Institute, ECE Dept.
Worcester, MA, USA
pedersen@wpi.edu

T. L. Szabo
Boston University, BME Dept.
Boston, MA, USA
tlszabo@bu.edu

Abstract— **Freehand 3D ultrasound imaging has been growing in popularity. However, the unavoidable reconstruction errors introduced by freehand motion have limited its usefulness. To overcome this, freehand ultrasound systems have been augmented with external tracking sensors to produce accurate 3D images in mainly experimental settings, but these systems have yet to be accepted for general clinical use. In addition, the use of external tracking sensors limits the portability of the system.**

This paper presents a 5 Degree of Freedom, low cost, integrated tracking device for quantitative, freehand, 3D ultrasound. It uses a combination of optical and inertial sensors to track the position and orientation of the ultrasound probe during a 3D scan. These sensors can be attached to or contained completely within the ultrasound transducer. Stradwin 3D ultrasound software acquires 2D image frames from the ultrasound system and position and orientation data from the tracking system to generate 3D ultrasound images in real-time.

3D reconstruction performance was evaluated by freehand scanning cylindrical inclusions in a tissue mimicking ultrasound phantom. Different scan patterns were tested to provide performance data for errors introduced in individual degrees of freedom. 3D images were formed from the data with and without the use of the tracking information, and then manually segmented. The volume and surface accuracy of the segmented regions were then compared to the ground truth. The mean volume error was 3.84% with the position information and 18.57% without. The mean RMS surface error was .381 mm with the position information and .843 mm without.

Keywords-Freehand Scanning, 3D Imaging, Quantitative Ultrasound, 6 DoF Tracking, Telemedicine

I. INTRODUCTION

Three-dimensional (3D) ultrasound has become an increasingly popular medical imaging tool over the last decade. Imaging in 3D allows data to be visualized in ways that would not be physiologically possible with a 2D instrument and permits realistic surface rendering to aid in diagnostic decisions for some cases.

The primary methods for capturing 3D ultrasound data include freehand scanning with a 1D array, mechanically assisted scanning with a 1D array, and direct 3D acquisition using a stationary 2D array. With a few exceptions, such as cardiac scanning, freehand scanning is the method most commonly used in the clinical environment.

When creating a 3D image from a set of 2D images, the relative locations and orientations of the individual image frames must be known to create an accurate reconstruction. This is a fundamental problem for freehand 3D ultrasound because, without the aid of an external sensing device, the sonographer has the challenging task to maintain constant scan rate and transducer attitude and cannot employ the angle variation for a more complete image visualization.

Commercially available sensor systems for tracking transducer position and attitude during imaging include electromagnetic and optical triangulation systems. Both require external references. In a clinical setting, metals can affect the accuracy of electromagnetic sensor types. In the optical systems, the user must be careful not to obstruct the light beams.

The goal of this work is to create a low cost tracking system for freehand 3D ultrasound that is completely self-contained within the transducer and without the need for external references. Such a system will allow for more accurate 3D reconstructions by providing the information necessary to align the individual 2D image frames.

II. SYSTEM OVERVIEW

Fig. 1 is a block diagram of our freehand 3D ultrasound system. The ultrasound imaging system is a Terason 3000, with a 5 – 9 MHz linear array transducer that connects via the beamformer unit to the PC using a Firewire interface. This system utilizes a PC for controlling, acquiring, processing and displaying ultrasound data. Mounted on the probe is a sensor module consisting of an optical tracking sensor and a 3 axis MEMS gyroscope. A navigation computer processes the sensor data in real-time to provide tracking information to the PC. The Stradwin software [1,2], running on the PC, combines the B-scans from the Terason system with tracking information from the navigation computer, to provide real-time 3D ultrasound images.

Stradwin is a software tool for freehand 3D ultrasound acquisition and visualization that was developed by the Medical Imaging Group at Cambridge University in England. The software interfaces directly to Terason ultrasound

This research work was supported under Contract No. DAMD17-03-2-0006 from the *Telemedicine and Advanced Technology Research Center (TATRC).*

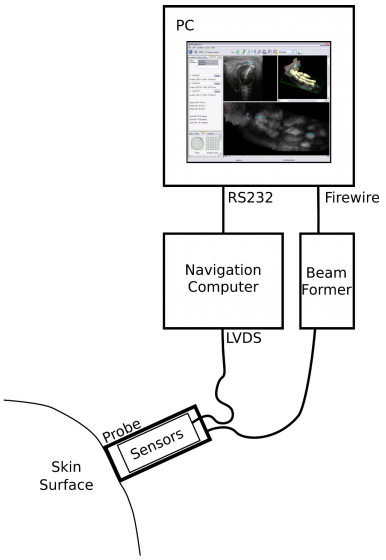

Figure 1. System Diagram, showing the transducer with the tracking sensors and the data flow from the transducer (probe) to ultrasound imaging system

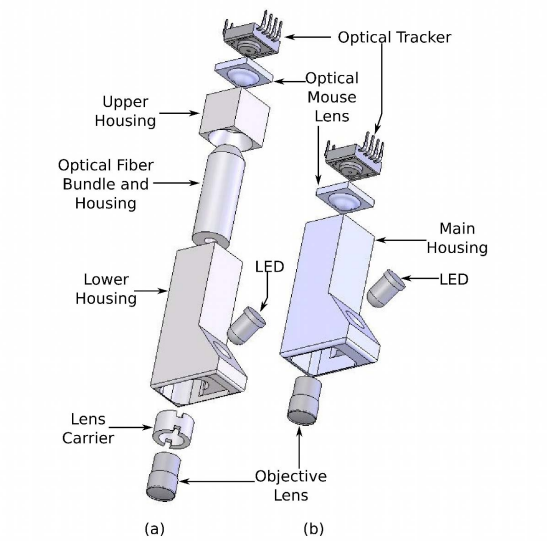

Figure 2. The transducer mountable optical trackers. (a) includes the optical fiber bundle and (b) does not.

transducers and to a number of commercial 6 Degree of Freedom (DoF) tracking systems. To interface our tracking system with the Stradwin software we emulated a commercial device. The unique visualization algorithms employed by Stradwin make it very fast, enabling real-time 3D visualization of data during acquisition and instant reslicing in any plane.

III. Optical Position Tracking

An optical mouse sensor is used to provide positional information along and orthogonal to the scan direction. The sensor consists of an 18x18 pixel CCD camera and a digital signal processor (DSP). The camera captures images at a rate of 1500 frames per second and the DSP computes the magnitude and direction of the motion based on the relative position of features between frames.

An initial evaluation of the optical mouse sensor's tracking performance used the sensor directly over the skin surface [3]. The evaluation revealed that the sensor, in its original design, is not well suited for tracking irregular surfaces such as human skin. There are two reasons for this. First, the optical mouse lens has only a 1 mm depth of field. When moving the sensor along the skin surface it is nearly impossible to control the distance between the lens and the skin that precisely. Second, features on the skin surface tend to be much larger than the surface features that the optical sensor was designed to track. This means that there are fewer features visible to the sensor and results in poor tracking.

To solve these problems, a second lens was added to the system. The original optical mouse lens had to be retained because there was no other lens available that could effectively focus the image through the small aperture in the image sensor. The second, or objective, lens was selected to have an increased depth of field at the cost of greater focal length. A 5 mm diameter miniature video camera lens was selected because of its compact size, short focal length, and low aberration. Because space inside the ultrasound transducer and next to the ultrasound array is very tight, we evaluated the option to include an optical fiber bundle in the system as well. Using an optical fiber, the objective lens could be mounted in the end of the transducer to focus light into the optical fiber. The image sensor and mouse lens could then be mounted at the other end of the fiber, where there would be more space available. For testing purposes, two prototype optical trackers were developed. One used an optical fiber, illustrated in Fig. 2(a), and the other, illustrated in Fig. 2(b), did not. Both were mounted to the ultrasound transducer externally, as illustrated in Fig. 4.

IV. Angle Sensing

A 6 DoF MEMS inertial sensor was used to sense angular rate of change. This sensor contains 3 orthogonally mounted linear accelerometers, 3 orthogonally mounted rate gyroscopes, and provides a digital interface to the sensor outputs. In the current implementation, only the gyroscopes are used.

Low cost angular rate gyroscopes such as this are generally not sensitive enough for inertial navigation. In addition, they suffer from initial bias and long term drift errors. Traditional inertial navigation systems calculate position by integrating the output of accelerometers twice. To do so, an estimate of the accelerometer's orientation must be used to compensate for the component of acceleration due to the earth's gravity. The sensitivity of the gyroscope is adequate for our system because we do not use the angle estimates for gravity correction. The initial bias is compensated for by recording the sensor output for 5 seconds at the beginning of each scan, while holding the probe still. The average value of the first 5 seconds of the sensor output is then subtracted from each subsequent sample.

V. Navigation Computer

The tracking system was implemented in a FPGA using a Microblaze soft-core embedded system. The XMK Real Time Operating System (RTOS) provided all of the basic software

services necessary to perform the system tasks. The system firmware was broken up into threads that were each responsible for an individual task. Each sensor has its own thread for sampling the raw data. Another thread implemented the navigation algorithm, which was responsible for transforming the raw sensor data into position and orientation data that Stradwin could use. Communication between the PC and the tracking system was managed by yet another thread.

The navigation computer used an inertial navigation algorithm to convert the individual sensor readings into an estimate of the transducer's position and pose. A Direction Cosine Matrix (DCM) was maintained to track the transducer pose. At the beginning of each scan it was initialized to the identity matrix and then evolved with each successive angular rate sample. The angular rate vector is formed from the turn rates about the x, y, and z axes, as in (1). In order to update the DCM, C_b^n, the matrix differential equation in (2) must be solved, where Ω_{nb}^b is a skew symmetric matrix formed from the elements of (1) [4].

$$\omega_{nb}^b = \begin{bmatrix} \omega_x & \omega_y & \omega_z \end{bmatrix}^T \tag{1}$$

$$\dot{C}_b^n = C_b^n \Omega_{nb}^b, \Omega_{nb}^b = \begin{pmatrix} 0 & -\omega_z & \omega_y \\ \omega_z & 0 & -\omega_x \\ -\omega_y & \omega_x & 0 \end{pmatrix} \tag{2}$$

Over a single cycle of the algorithm, (2) may be rewritten as (3).

$$C_{k+1} = C_k \exp \int_{t_k}^{t_{k+1}} \Omega_{nb}^b dt \tag{3}$$

Assuming that the angular rate vector, ω_{nb}^b, remains fixed over the update interval, the integral in (3) can be expressed as (4). This assumption remains valid as long as the update interval remains small.

$$\int_{t_k}^{t_{k+1}} \Omega_{nb}^b dt = [\sigma \mathrm{x}], [\sigma \mathrm{x}] = \begin{pmatrix} 0 & -\sigma_z & \sigma_y \\ \sigma_z & 0 & -\sigma_x \\ -\sigma_y & \sigma_x & 0 \end{pmatrix} \tag{4}$$

Equation (3) can now be restated as the product of two DCMs as given in (5). The matrix $\mathbf{C}_k$ is the DCM that relates the body reference frame to the navigation reference frame at time *k*, and $\mathbf{A}_k$ is the DCM which transforms a vector in the body reference frame at time *k+1* to the body reference frame at time *k*.

$$C_{k+1} = C_k \exp[\sigma \mathrm{x}] = C_k A_k \tag{5}$$

To solve (5), $\mathbf{A}_k$ is approximated by a fourth order Taylor series.

To make the algorithm as fast as possible, all of the constant values were pre-computed and stored as constants. In addition, the processor we used did not include a floating point divider, so many of the coefficients were stored as reciprocals to avoid slow software division routines.

The optical tracker reported linear displacement relative to a coordinate system fixed to the ultrasound transducer. This coordinate system is known as the body reference frame. In order to track the position of images in a sequence, their positions must be measured relative to the first image in the series. The coordinate system centered on the first image is known as the navigation reference frame. The position of each subsequent image is represented as a translation and a set of rotations relative to the first image. The linear displacement measured by the optical tracker in the body reference frame is represented as a vector in (6). The z component is always zero because this system has no way of measuring along that axis. This vector is transformed into the navigation reference frame by multiplying it by the DCM, C_b^n, resulting in (7). The coordinates of the probe in the navigation reference frame are updated after each new position sample by adding the result of this transformation to a running sum for each axis.

$$r^b = [d_x \quad d_y \quad 0] \tag{6}$$

$$r^n = C_b^n r^b \tag{7}$$

VI. Performance Evaluation

The quantitative 3D ultrasound scanning system was tested by scanning a cylindrical inclusion in a CIRS model 044 ultrasound phantom. The CIRS phantom contained several inclusions of varying shapes and sizes. The inclusion used for testing was cylindrical with a length of 18 mm and a diameter of 12 mm, as illustrated in Fig. 3. The inclusion had a scattering level of -6 dB with respect to the surrounding material. For testing purposes the shape of the inclusion was assumed to be an ideal cylinder.

Five different tests were devised and 10 trials of each test were conducted. The entire test series was repeated for the versions of the tracking system with and without the optical fiber. The *first test* consisted of linear motion along the y axis while maintaining as uniform a rate and angle as possible. In the remaining tests, all but one variable were kept as constant as possible. The *second test* consisted of linear motion along the y axis at a variable rate. The *third test* consisted of linear motion along the y axis combined with back and forth linear motion along the x axis. The *fourth test* consisted of linear motion along the y axis combined with positive and negative pitch variation. The *fifth test* consisted of linear motion along

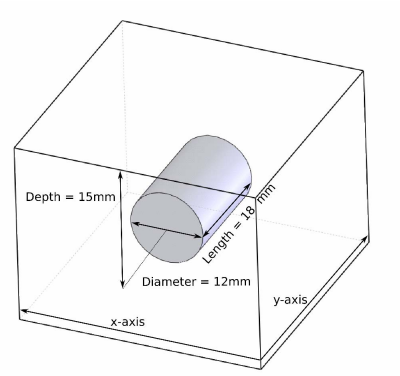

Figure 3. Diagram of the section of the CIRS 044 ultrasound phantom used for testing.

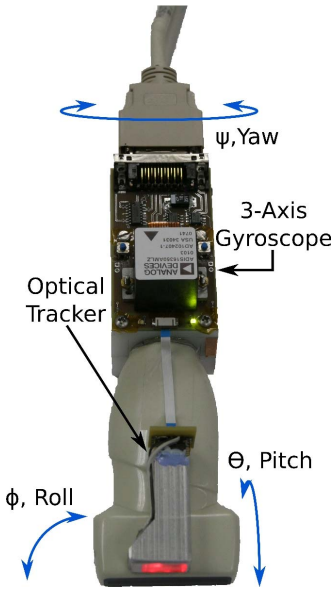

Figure 4. The prototype tracking hardware attached to the ultrasound transducer. The blue lines indicate the yaw, pitch, and roll axes.

the y axis combined with positive and negative yaw variation. It is important to note that all of the tests were performed by hand. Therefore, there was always some motion present in each degree of freedom. The linear degrees of freedom are defined in Fig. 3. The rotational degrees of freedom are defined in Fig. 4.

Volume error and surface error were used as the performance metrics. After the datasets were recorded, the inclusion was manually segmented using the utilities provided within the Stradwin program. Each segmentation was performed with and without the position information, in order to provide a basis for comparison. The segmentations in Fig. 5 are representative of the segmentation results. Figs. 5 (a) and (b) are from a dataset where the pitch angle was varied during the scan. The segmentation in Fig. 5 (a) makes use of the tracking information, while the segmentation in (b) does not. Figs. 5 (c) and (d) are from a dataset where variation was present in the x linear dimension. Fig. 5 (c) makes use of the tracking data while (d) does not.

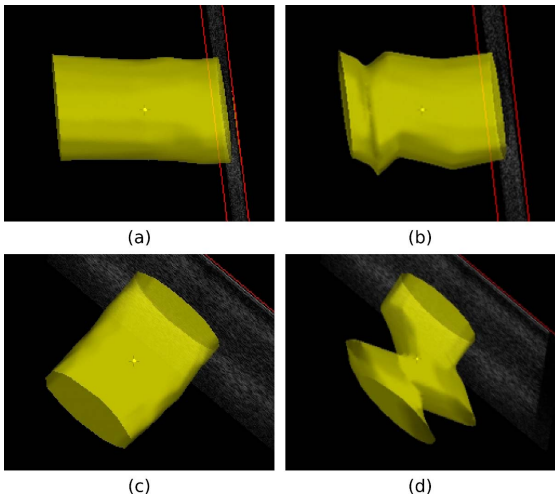

Figure 5. (a) Volume segmentation of a data set with pitch variation using tracking information and (b) not using tracking information. (c) Volume reconstruction of a data set with linear variation in the x dimension using tracking information and (d) not using tracking information.

The volume of the segmented region is calculated automatically by Stradwin. The volume error was calculated as the absolute value of the difference between the segmented volume and the ground truth volume, divided by the ground truth volume.

Although volume error is a useful metric, it does not reveal surface errors. It is quite possible for two very different 3D segmentations to have similar volumes. The surface accuracy metric characterizes the degree of similarity between two objects by comparing the RMS distance between points on their respective surfaces. The two surfaces are first aligned using the Iterative Closest Point (ICP) algorithm [5]. The IPC algorithm finds the affine transformation between the two point sets that minimizes the distance between points in the segmentation result and the ground truth in the least squared sense. The transformation is then applied to the data. To compute the surface accuracy, the Euclidean distance from every point in the segmentation result to every point in the ground truth point set is calculated and the smallest one is recorded. The RMS value of this collection of distances between the surfaces is then calculated [6].

VII. Results

A. *Volume Error*

The volume error results are presented in Fig. 6 for the version of the tracking system that did not incorporate the optical fiber and in Fig. 7 for the version that did. Each group, 1 to 5, along the x axis represents one of the five tests (or motion profiles) described in Section VI. For the version of the system without the fiber (Fig. 2b), the mean volume error was 3.84% with a std. dev. of 1.58% across all tests versus 18.57% with a std. dev. of 2.72% without the position information. For the version of the system that included the optical fiber (Fig. 2a), the mean volume error was 5.59% with a std. dev. of

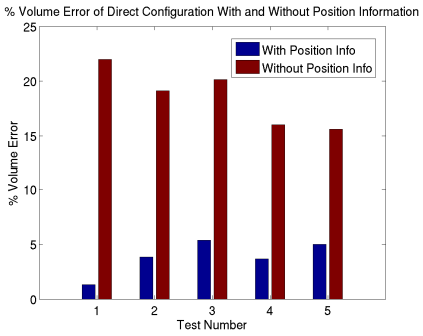

Figure 6. Comparison of volume error with and without position information for system without optical fiber.

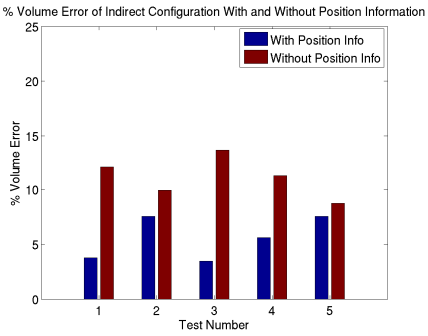

Figure 7. Comparison of volume error with and without position information for system with optical fiber

1.97% across all tests versus 11.16% with a std. dev. of 1.92% without the position information.

B. *Surface Error*

The surface error results are presented in Fig. 8 for the version of the tracking system that did not incorporate the optical fiber and in Fig. 9 for the version that did. Each group along the x axis represents one of the five tests (or motion profiles) described in Section VI. For the version of the system without the fiber, the mean RMS surface error was .381 mm with a std. dev. of .056 mm versus .843 mm with a std. dev. of .236 mm without the position information. For the version of the system with the fiber, the mean RMS surface error was .486 mm with a std. dev. of .170 mm versus .813 mm with a std. dev. of .476 mm without the position information.

VIII. Conclusion

The prototype system successfully demonstrated that accurate 3D ultrasound volumes can be generated from 2D freehand data using only sensors integrated into the ultrasound probe. Both versions of the system significantly improved reconstruction accuracy. The version without the optical fiber outperformed the version with the optical fiber in all cases. The main drawbacks of this system are that it does not provide full 6 DoF tracking data and that the scan duration is limited due to drift in the gyroscopes. Future work should focus on finding a way to sense linear displacement along the z-axis and improved methods for drift compensation.

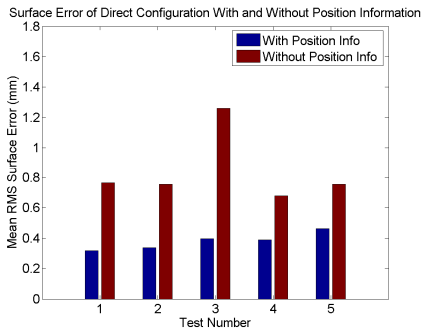

Figure 8. Comparison of RMS surface error with and without position information for system without optical fiber

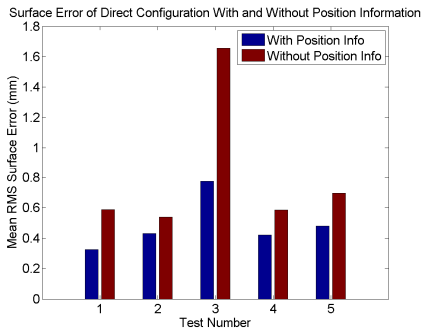

Figure 9. Comparison of RMS surface error with and without position information for system with optical fiber

Acknowledgment

The authors acknowledge the technical support of the developers of Stradwin, who provided technical guidance and a specially modified version of the software to aide our development. In addition, we acknowledge *CIRS* inc. for lending us the model 044 ultrasound resolution phantom and *Terason* Inc. for technical assistance. The financial support of the *Telemedicine and Advanced Technology Research Center* is gratefully acknowledged.

References

[1] G. Treece, R.W. Prager, and A.H. Gee. The Stradwin 3D Ultrasound Acquisition and Visualization System. http://www.eng.cam.ac.uk/~rwp/stradwin/.

[2] R. W. Prager, A. H. Gee and L. Berman. “Stradx: real-time acquisition and visualization of freehand three-dimensional ultrasound,” *Medical Image Analysis*, 3(2):129.140, 1999.

[3] C. Poulsen, P. C. Pedersen, and T. L. Szabo, An optical registration method for 3D ultrasound freehand scanning, Proceedings of the IEEE 2005 Ultrasonics Symp., (0-7803-9383-X/05, IEEE New York), pp1236-1240.

[4] D. H. Titterton and J. L. Weston, Strapdown Inertial Navigation Technology. American Institute of Aeronautics and Astronautics, Inc. 2004

[5] P. Besl and N. McKay, “A method for registration of 3-d shapes,” IEEE Transactionson on Pattern Analysis and Machine Intelligence, vol. 14, no. 2, pp. 239–256, 1992.

[6] J.D. Quatararo, “Semi-automated segmentation of 3d medical ultrasound images,” Master’s thesis, Worcester Polytechnic Institute, 2008.